Accepted Manuscript

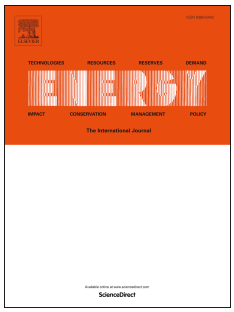

High solar photovoltaic penetration in the absence of substantial wind capacity: Storage requirements and effects on capacity adequacy

Fabrizio Fattori, Norma Anglani, Iain Staffell, Stefan Pfenninger

PII: S0360-5442(17)31181-7

DOI: 10.1016/j.energy.2017.07.007

Reference: EGY 11194

To appear in: *Energy*

Received Date: 31 January 2017

Revised Date: 28 June 2017

Accepted Date: 1 July 2017

Please cite this article as: Fattori F, Anglani N, Staffell I, Pfenninger S, High solar photovoltaic penetration in the absence of substantial wind capacity: Storage requirements and effects on capacity adequacy, *Energy* (2017), doi: 10.1016/j.energy.2017.07.007.

High Solar Photovoltaic Penetration in the Absence of Substantial Wind Capacity: Storage Requirements and Effects on Capacity Adequacy

Abstract

The penetration of solar photovoltaic (PV) generation is increasing in many countries, with significant implications for the adequacy and operation of power systems. This work considers the Nord bidding zone within Italy, which hosts 7.7 GW of PV and almost no wind power. We simulate the implications of different PV penetration levels on the need for firm generation capacity and on ramping requirements over one to several hours. We compare ten years of synthetic hourly PV generation series derived from CM-SAF SARAH satellite data and observed load. The analysis also provides insights into the storage capacity required to smooth residual load over different time horizons. Results show that without storage (i) the penetration of PV in the region does not sensibly reduce the need for firm generation; (ii) the marginal contribution of PV to meet power demand decreases with its penetration; and (iii) high penetrations lead to larger and more frequent ramps, although extreme ramp rates do not last more than one hour. The availability of storage significantly alters these results, but large storage capacities are required. Smoothing net load by a few hours requires 2-7 GWh of storage per GW of PV installed.

Keywords: Solar Energy, Electricity Storage, Capacity Adequacy, Power system, Solar PV, Ramp Rate

1. Introduction

The share of photovoltaics (PV) in power generation capacity is rapidly increasing in many countries worldwide. In just a few years, it has reached a

cumulative installed capacity of 303 GW_P as of 2016 [1].

Due to a feed-in tariff from 2005 to 2013, Italy in particular has seen a strong growth in PV. Though the growth trend has ended after the tariff stopped in 2013, Italy reached a cumulative installed capacity of 19.3 GW_P as of 2016, giving it the worlds fifth-largest installed capacity [1]. While increasing PV penetration helps to decarbonise the power system, it also brings new challenges to its planning and management [2, 3]. PV is a variable electricity source which is still challenging to accurately forecast, influenced by factors such as the absence of irradiance at night, the dependence on seasons and cloud cover, and even astronomical events such as solar eclipses [4]. Backup generation and/or storage capacity are needed to supply power to the grid when PV is not available or when actual generation differs from the forecast. Backup solutions must be ready and able to ramp up and down[1] rapidly enough to handle the fluctuations of PV [3]. This need to balance variable generation means that fossil-fired firm generation capacity is now being operated in originally unintended ways, with reduced utilisation and increased cycling, which in turn affects average efficiencies, emission factors and eventually costs [6, 7, 2]. The impact of high shares of PV on firm generation can be divided into two categories, each related to a different temporal resolution: (i) the problem of capacity adequacy, which we define as the ability to provide the power required by the system under steady state conditions, throughout the year, with a given probability and (ii) the problem of system security, which we define as the ability to cope with dynamic and unplanned load changes, with a given probability of preserving the nominal voltage and frequency of power. While the first can be studied with hourly resolution, the second needs finer temporal detail. They are not however completely independent, since some of the capacity that contributes to adequacy is also used to provide voltage and frequency regulation services

[1] After [5], we define ramping as the changing of residual load over time (upward and downward), and thus in output from non-PV generators, expressed in GW over the reference periods.

(by offering a margin to increase or decrease its load factor or through rotating inertia).

These two dynamics depend on the load profiles, climate conditions, and the size and geographical location of a particular power system. Here we focus on the northern bidding zone of the Italian electricity market, called *Nord*, an area of about 120 000 km^2 and 28 million inhabitants with about 7.7 GW$_P$ of PV as of 2016 [8]. One feature of the Nord zone is its limited potential for wind power. It thus presents an ideal case study for analysing the impact of PV in isolation since there cannot be the possible mitigating effect generally offered by wind power [2].

We analyse how different penetration levels of PV would impact the firm generation under steady-state conditions, focusing on the capacity adequacy problem. This is done by looking at two metrics: (i) the amount of firm capacity that PV can replace while maintaining system adequacy, and (ii) the flexibility (in terms of ramping capabilities) that is required for firm generation to deal with the variability of PV. Both issues are investigated assuming different scenarios for storage potential in the power system.

This work strengthens a previous analysis [9] which considered a circumscribed part of the bidding zone and used one year of data coming from a limited number of irradiance measuring stations and a simple projection of the national load profile. Here, time series of ten consecutive years are considered, from 2006 to 2015, with improved modelling of PV generation thanks to the use of gridded satellite irradiance data. The analysis considers a wider range of PV penetrations, considers the potential role of storage, and analyses ramps over timespans longer than one hour.

1.1. State of the Art

There is only a limited amount of literature studying the reliability and effectiveness of PV in absence of substantial amounts of wind generation, as the two are usually analysed together. Past work has studied the problem in terms of *capacity credit* [10, 11, 12, 13, 14], *power value* [15], *effective capacity* [16],

potential in reducing the demand [17], and dispatchable generation that PV can replace [18].

The methods for estimating the capacity value of solar power have been also reviewed by an IEEE Task Force [19] very recently. Since all the mentioned studies were conducted for different penetration levels, in different case studies, with different spatial scales and with different methods, their results cannot be directly compared. It is possible however to detect a common trend: due to its variability, particularly the day-night cycle, the marginal ability of PV to contribute to meeting load decreases as its penetration increases towards a certain limit.

The literature on capacity adequacy has only recently started considering the implications of PV penetration on flexibility requirements. The focus has been on long-term ramps, namely the variations of load, net of PV generation, that occur within a time span of one or more hours. Relatively few studies exclusively cover PV power [14, 9, 20, 21] as most consider PV within the mix of variable renewable sources [5, 22, 2, 23]. These studies show a common trend: with lower penetrations, ramps are defined by the load; after a critical level, ramp rates increase with the penetration of PV.

Several studies have analysed the relationship between PV penetration and long-term storage [24, 25, 26, 14, 27, 21]. PV penetration is usually analysed in relation to the storage requirements that are needed to reach given targets, for example, reducing fluctuations in load, reducing unusable energy, increasing capacity credit, or reducing ramps. Understanding these PV-storage relationships depends on two main features: (i) the ratio between energy and power capacity of the storage technology and (ii) the storage horizon considered (intra-daily, weekly, seasonal, etc.). The common approach is either (i) to take fixed assumptions for these two features in order to analyse the effect on the power system or (ii) to determine these two features as results of the analysis assuming a given behavior of the power system. In our analysis we fix different horizons, from three hours up to monthly, and let the energy-to-power ratio result from the analysis while varying the penetration of PV.

Throughout the literature there is no common definition of the term *penetration*. It is usually considered in two ways: (i) installed PV capacity relative to peak load, or (ii) annual energy generated by PV relative to annual energy demand. Here, we use the second definition. Annual demand within Nord is around 165 TWh with a peak of around 29 GW. Thus, the overall system has an average utilisation of 64% - solar PV in the region averages a capacity factor of 12%, meaning that capacity penetration is more than 5 times higher than energy penetration. By using the second definition of penetration, it is thus more challenging to reach higher degrees of penetration. It must be pointed out that only some of the studies cited above took into account very high levels of PV penetration [15, 14, 21, 24, 7, 26, 27, 23]. This study goes beyond past work to examine a wide range of PV penetration, including covering almost the entire annual energy demand with PV.

2. Methods

We study the implications that different levels of PV penetration would have on the capacity adequacy needs of the northern bidding zone of the Italian electricity market, called *Nord*, with and without storage. As in other Italian bidding zones, Nord has no practical transmission limits within its boundaries, and we assume this remains valid with the increased PV penetrations we analyse[2]. We therefore model generation and demand within Nord as a single bus.

The analysis is based on ten years of historical weather conditions and demand data to cover a variety of conditions and capture infrequent extremes. We do not provide scenarios describing installed PV capacity at a specific point in the future, as this work is meant to be used within capacity expansion models, where installed capacity is an endogenous variable. This work generically focuses on the load that is not met by PV, which we call *residual load*[3].

[2] We also assume that no other technical or socio-economic issues limit the penetration of PV (distribution networks are improved, installed PV does not compete for land use, etc.)

[3] residual load is also called *net demand* or *net load* in other studies

Table 1: Indexes used in the equations

t	time steps of one hour; within the used data-series each t refers to a particular historical hour, from t=1 to t=87648 respectively representing the first hour of January 1st 2006 and the last hour of December 31st 2015)
k	same as t; it is used in some equations together with t in order to differentiate the domain that different parts of the equations refer to
l	levels of penetration of PV generation capacity within the generation portfolio of the considered area. A detailed definition is provided in Section 3.1
m	time spans of ramps; the index refers to the number of hours between the two loads that are considered to calculate the slope
n	time spans of the storage strategies; the index refers to the number of hours that are considered for averaging the load in a generic time step

In this section we provide the equations that define the time series of residual load and its ramps (Section 2.1). We then describe the method used for building time series of the residual load after simulating different storage strategies (Section 2.2). Tables 1 and 2 describe the indices and variables used in the equations.

2.1. Residual Load and Ramp Rates

The residual load (RL) is the difference between the load profile and the PV generation profile at a given time:

$$RL_{t,l} = L_t - PVg_{t,l} \tag{1}$$

where t is the time step the measure refers to; the index l indicates the PV penetration level (defined later); L_t is the demand load at the same time step and $PVg_{t,l}$ is the potential PV generation output at the same time step and under the same *l-th* penetration level.

Studying the time series of residual load and its ramps allows us to specify the requirements that non-PV generation capacity must fulfil. Because of the correlation between PV generation and electricity demand, it is important that the two series of data used in equation (1) cover the same historical period. This issue will be further discussed in Section 3.

Table 2: Variables used in the equations

$PVg_{t,l}$	Simulated power output resulting from aggregating the PV plants in the considered area
$PVcap_l$	Peak capacity that is assumed for the PV plants installed in the considered area
CF_t	Aggregated hourly capacity factor of PV for the considered area
$RL_{t,l}$	Residual load (load that is not covered by PV plants)
$RLC_{t,l}$	Residual load (load that is not covered by PV plants) net of excess energy
$DL1_{t,l,n}$	Desired load resulting from the simulation the storage strategies (first step)
$DL2_{t,l,n}$	Desired load resulting from the simulation the storage strategies (second step)
$RR_{t,l,m}$	Ramp rates (difference between two values of the residual load)
L_t	Load that must be met by the generation capacity (be it conventional or renewable)
$\Delta PS1_{t,l,n}$	Power that is coming from or going to the storage (first step)
$\Delta PS2_{t,l,n}$	Power that is coming from or going to the storage (second step)
$BSE1_{t,l,n}$	Cumulative balance of the energy that has come or has left the storage (first step)
$BSE2_{t,l,n}$	Cumulative balance of the energy that has come or has left the storage (second step)
η_{ch}	Average charging efficiency of the storage facilities
η_{dis}	Average discharging efficiency of the storage facilities
$APS_{t,l,n}$	Additional power that must be provided to the storage systems to balance losses
$CPC_{l,n}$	Overall charging power of the storage facilities
$DPC_{l,n}$	Overall discharging power of the storage facilities
$ASE_{t,l,n}$	Amount of energy that is stored in the storage facilities
$ESC_{l,n}$	Overall energy storage capacity of the storage facilities

The residual load as calculated above does not provide any information on the amount of excess energy that would be wasted unless stored. A different time series of residual load is necessary to quantify and then exclude waste energy from the analysis:

$$RLC_{t,l} = \begin{cases} RL_{t,l} & \text{if } RL_{t,l} > 0 \\ 0 & \text{if } RL_{t,l} \leq 0; \end{cases} \tag{2}$$

where $RLC_{t,l}$ is the residual load net of excess energy.

Ramp-ups and ramp-downs of RLC are analysed in order to detect the ramping requirements that the non-PV generation capacity must fulfill. Unlike in [9], and similarly to [23], the ramps of RLC are calculated for various levels of PV penetration considering different time spans, ranging from one to several hours. Quantifying the ramping over different time spans allows differentiation between the need for short-term flexibility (units that can provide extreme ramps for one hour), and longer-term balancing (those that must sustain such a slope for two or more hours).

The *m-hour* ramp rates (RR) are calculated for each *t-th* hour as the difference between the RLC in that same *t-th* hour and the RLC of the hour *t-m*, as in:

$$RR_{t,l,m} = RLC_{t,l} - RLC_{t-m,l} \qquad \forall t > m \tag{3}$$

2.2. Storage Simulations

For each level of PV penetration we simulate the residual load profile under different storage potentials. Simulating the use of the storage facilities without knowledge of the installed generation capacity or market prices is challenging because these are important factors in real-world operational decisions, whether storage units are managed by the market or an independent operator. Our simulations are based on the assumption that storage potential will be used to smooth peaks and valleys and to reduce lost energy.

The analysis assumes perfect foresight, that is, all operators have a full knowledge of the loads and of PV generation until the end of the time horizon taken into account by the different storage strategies (see below for the definition of these strategies). System inefficiencies due to forecasting uncertainty are not considered, and so results can be seen as a benchmark defining the best possible scenario.

A further important consideration is that storage is modelled as a single aggregated unit, so our results do not consider where storage might be located and how many facilities would be needed. As we model Nord as a single bus, we assume that all storage facilities are connected to the grid and optimally interact with it through a perfect market, or are optimally managed by a central independent operator (stand-alone combined PV and storage systems might exist, but are not taken into account by the analysis).

Two sequential steps are used to simulate the storage strategies: a first step which calculates the base dispatch excluding charging losses, and a second step which accounts for device inefficiency. The two steps are described in the next two subsections.

2.2.1. First simulation step

Similarly to the approach of Weiss et al. [26], storage strategies are first simulated by means of central moving averages: in each *t-th* hour the desired load net of storage ($DL1_{t,l,n}$) is the average value of the residual load ($RL_{z,l}$) of a given n number of hours in the neighbourhood of the *t-th* hour, as in:

$$DL1_{t,l,n} = \frac{\sum_{z=t-(n-1)/2}^{z=t+(n-1)/2} \cdot RL_{z,l}}{n} \qquad \forall n = 2k+1 : k \in \mathbb{N} \tag{4}$$

As an example, a 3-hour storage strategy ($n = 3$) means that, in each hour, the resulting value of $DL1_{t,l,n}$ is the average of the *t-1*, t and *t+1* values of $RL_{t,l}$. The wider the considered interval, the smoother the peaks, the valleys and the ramps of the desired load (DL) profile compared to the residual load (since extreme values are distributed over more hours). The calculated load profiles can thus be considered as the residual load of the system with a certain

amount of storage which allows non-PV generation to meet demand. Varying the n index within an analysis allows us to quantify the relationship between the storage strategy (timespan of net-load smoothing) and its effects on the power system. This method does not take into account economic or technical feasibility, but shows the required magnitude of storage. For each *n-th* strategy, the power exchanged between storage and grid in each hour ($\Delta PS1_{t,l,n}$) is the difference between desired load and residual load in that hour:

$$\Delta PS1_{t,l,n} = DL1_{t,l,n} - RL_{t,l}. \tag{5}$$

When $\Delta PS1_{t,l,n}$ is positive, storage is charged from the grid, and vice versa. The charging and discharging power required in each hour by the storage to *transform* $RL_{t,l}$ into $DL1_{t,l,n}$ can be summed up until the end of the horizon net of the charging and discharging efficiencies, providing the balance of stored energy $BSE1_{t,l,n}$ as

$$BSE1_{t,l,n} = BSE1_{t-1,l,n} + \begin{cases} \Delta PS1_{t,l,n} \cdot \eta_{ch} \cdot \Delta t & \text{if } \Delta PS1_{t,l,n} > 0 \\ \Delta PS1_{t,l,n} \cdot \eta_{dis}^{-1} \cdot \Delta t & \text{if } \Delta PS1_{t,l,n} < 0 \end{cases} \quad \forall t > 1; \tag{6}$$

where Δt is the time span between two consecutive time steps t (in our case 1 hour); η_{ch} and η_{dis} are the average charging and discharging efficiencies of the storage facilities; and $BSE1_{0,l,n} = 0$.

2.2.2. Second simulation step

The second step is required to take into account charging losses. Here we compute the final desired load profile (DL2) from the preliminary profile (DL1) described above.

The last value of the $BSE1_{t,l,n}$ series ($BSE1_{t=T,l,n}$), when multiplied by the charging efficiency, indicates the amount of energy that is lost due to the charging efficiency. This amount must be additionally generated and stored. We simulate this by assuming that the additional amount of energy is distributed

over the $DL1_{t,l,n}$ profile through a proportional criteria, as in the equation

$$APS_{t,l,n} = \frac{-BSE1_{T,l,n}}{\eta_{ch}} \cdot \frac{\max_1^T DL1_{t,l,n} - DL1_{t,l,n}}{\left(\max_1^T DL1_{t,l,n} \cdot \Delta T\right) - \sum_{k=1}^{k=T} DL1_{k,l,n}} \quad (7)$$

where $APS_{t,l,n}$ is the additional power that must be stored to balance charging losses in each *t-th* hour. The last term of equation 7 prevents the additional power, APS, from increasing existing peaks, as depicted in Fig.1. We now

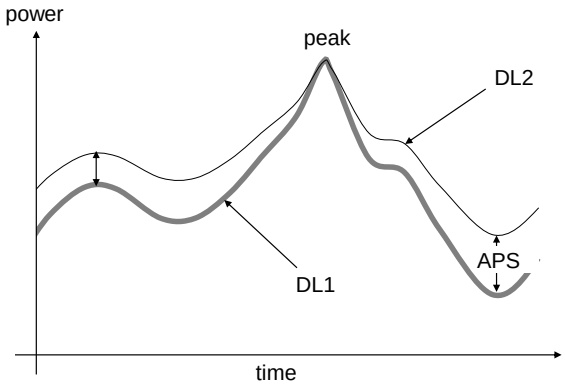

Figure 1: Qualitative description of how the additional energy required by the storage facilities (due to losses in the charge process) is distributed over the preliminary profile (DL1) to generate the final profile (DL2): the additional power (APS) is higher when close to the valleys and zero at the peak.

compute the final *n-th* desired load ($DL2_{t,l,n}$) by adding the $APS_{t,l,n}$ profile to the *n-th* desired load from the first step ($DL1_{t,l,n}$) (see Fig.1):

$$DL2_{t,l,n} = DL1_{t,l,n} + APS_{t,l,n}. \quad (8)$$

At this point, the power exchanged between storage and the grid in each *t-th* hour to reproduce the profile under the *n-th* storage strategy is calculated as the difference between the *n-th* strategy load profile and the load profile without storage ($RL_{t,l,n}$):

$$\Delta PS2_{t,l,n} = DL2_{t,l,n} - RL_{t,l}. \quad (9)$$

In this second step the balance between the stored energy and the energy provided by the storage facilities results from the balance calculated in the first iteration ($BSE1_{t,l,n}$) increased by the additional energy provided up to that same hour to balance the losses:

$$BSE2_{t,l,n} = BSE1_{t,l,n} + \sum_{k=1}^{k=t} APS_{k,l,n} \cdot \Delta t. \tag{10}$$

To assess the amount of stored energy in the storage facilities ($ASE_{t,l,n}$) in each *t-th* hour the $BSE2_{t,l,n}$ must be increased by a quantity that equals its lowest value within the series and that represents the initial amount of energy stored in the facility:

$$ASE_{t,l,n} = BSE2_{t,l,n} + \min_{1}^{T} \left(BSE2_{t,l,n}\right); \tag{11}$$

From the two steps outlined above, we can derive power and energy capacity of the storage facilities. The lowest and the highest values of $\Delta PS2_{t,l,n}$ over the entire horizon provide the overall charging power capacity ($CPC_{l,n}$) and discharging power capacity ($DPC_{l,n}$) required to comply with a given *n-hour* strategy, respectively:

$$CPC_{l,n} = \max_{1}^{T} \Delta PS2_{t,l,n} \tag{12}$$

$$DPC_{l,n} = \min_{1}^{T} \Delta PS2_{t,l,n} \tag{13}$$

The highest value of ASE provides the storage capacity ($ESC_{l,n}$) required to fulfill the *n-hour* storage strategy requirements.

$$ESC_{l,n} = \max_{1}^{T} \left(ASE_{t,l,n}\right). \tag{14}$$

3. Data

To ensure the representativeness of data, three factors are important: (i) time series length, since load and PV generation vary from year to year; (ii)

spatial resolution, since load and PV generation vary from place to place; (iii) the temporal correlation between the time series of load and generation, given that both depend on meteorological conditions such as irradiance and temperature. The analysis is based on ten years of data (2006-2015). While the potential PV generation data is available from 1986 on, the limited availability of load data limits our overall analysis to these ten years. Section 3.1 describes the hourly PV capacity factors and section 3.2 the hourly load series.

Data on PV capacity factors and load series are openly available at `https://www.renewables.ninja/downloads?pub=egy-17-italyf` and at `https://zenodo.org/record/818172` respectively.

3.1. PV Generation Time Series

To simulate PV output, we use the installed capacity in each of the 3,425 municipalities within Nord as of October 2016, obtained from [8]. Fig. 2 shows the spatial distribution of PV capacity in the Nord region. As production data

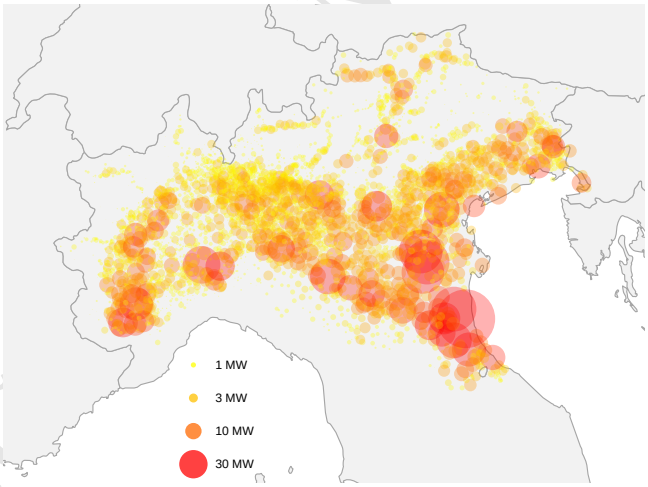

Figure 2: Spatial distribution of PV capacity in the Nord bidding zone (as of October 2016).

are not available from [8], we also gathered power production data alongside metadata such as location, installed panel capacity and panel angles for 185 PV installations from the PVOutput database, as described in [20]. The CM-SAF

SARAH dataset [28, 29] was used to simulate the hourly power output from 1986 to 2015 from each municipality using the Global Solar Energy Estimator model [20], using panel alignments drawn randomly from normal distributions describing the PVOutput metadata (Tilt: mean 15 ± 12 degrees; Azimuth: mean 183 ± 47 degrees). The measured panel output data was used to determine systematic bias in the simulations, by comparing measured with modelled time series. Based on this, the simulations were multiplied by a correction factor of 0.86, giving an R-squared for day-averaged time series of 99%. At the hourly resolution, the root mean square (RMS) error was 3.3%, implying that a modelled capacity factor of 0.45 in a given hour is accurate to within a range of 0.417-0.483 [20]. Fig.3 shows a comparison of the mean weekly capacity factor from the 185 measured panels and our corrected simulation. This bias correction

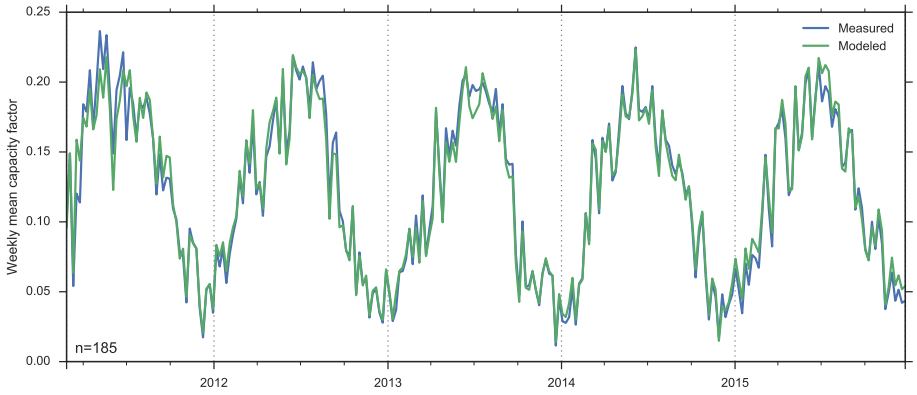

Figure 3: Comparison of the mean weekly capacity factor from the 185 measured panels and our corrected simulation

was applied to the municipality-level simulations. They were then aggregated to the entire Nord region by a capacity-weighted mean, resulting in a single time series of hourly capacity factors, CF_t. Fig.4 shows its variability (annual maximum and annual mean) throughout the period 1986-2015.

Since the analysis covers different levels of PV penetration, the aggregated hourly capacity factor was multiplied by the installed capacity assumed for each

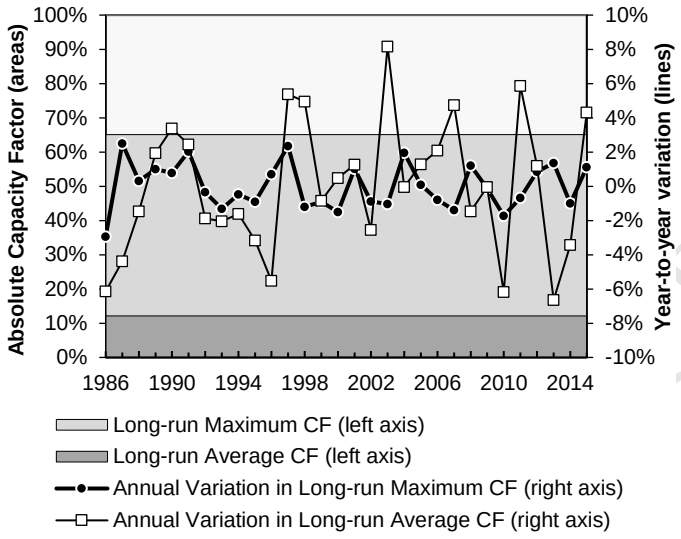

Figure 4: Annual variability of the capacity factor, assuming PV capacity installed in the region follows the current spatial distribution, for historical weather conditions from 1986-2015.

l-th level, $PVcap_l$, to obtain the series of PV generation, as in:

$$PVg_{t,l} = PVcap_l \cdot CF_t \tag{15}$$

The analysis assumes the spatial distribution shown in Fig. 2 remains constant for the different penetration levels. 14 levels of penetrations were considered, from the absence of PV (penetration = 0%; 0 GW_P) up to an installed capacity able to generate the average annual demand of the region, based on 1986-2015 (penetration = 100%; 155.8 GW_P). We considered steps of 10% between the penetration levels, with smaller steps at lower penetrations to better observe the dynamics close to the current installed capacity. Using our definition of penetration, the current installed capacity in the region is about 5% (7.8 GW_P). Assuming an average occupation of 10 m^2 per installed kW_P, a penetration of 100% implies covering 1558 km^2 of surface area, which is 1.3% of the regions total area. This percentage, though high, is about the same order

of magnitude as the 923 km^2 [30] used by industry and commercial settlements in the Lombardy Region alone (the Lombardy Region is one fifth of the total area of the Nord zone). We thus assume 100% PV penetration is feasible from a land-use perspective.

3.2. Load Time Series

Load data come from two sources: (i) Terna (the Italian TSO) provides load series detailing the six bidding zones of the Italian electricity market for a limited number of years (2010-2015) [31]; (ii) ENTSO-E (the European Network of Transmission System Operators) provides longer time series (2006-2015) of national aggregated load [32]. We combine these to give a synthetic 10-year time series for Nord (2006-15). In the appendix A, we describe the construction of this synthetic time series, including how erroneous values were corrected, missing values were filled and how we applied a regression between national and Nord demand.

4. Results and discussion

Results are presented in two subsections. In section 4.1 we focus on peaks, ramps and excess energy to analyse the most challenging situations for the power system under steady state conditions, for given likelihoods of occurrence. In Section 4.2 we discuss how storage can reduce the impact or frequency of those situations. The derived results are openly available at `https://zenodo.org/record/818172`.

4.1. Peaks, ramps and excess energy

The analysis of residual load and its ramps focuses on detecting extreme values and their likelihood of occurrence. In particular, we examine the maximum and minimum values, and different percentiles that represent frequencies of occurrence: once in ten years, once per year, ten times per year, once per day.

Some additional percentiles are considered to provide a more complete overview of the dynamics.

Fig.5 summarises residual load over the modelled ten years. Residual load

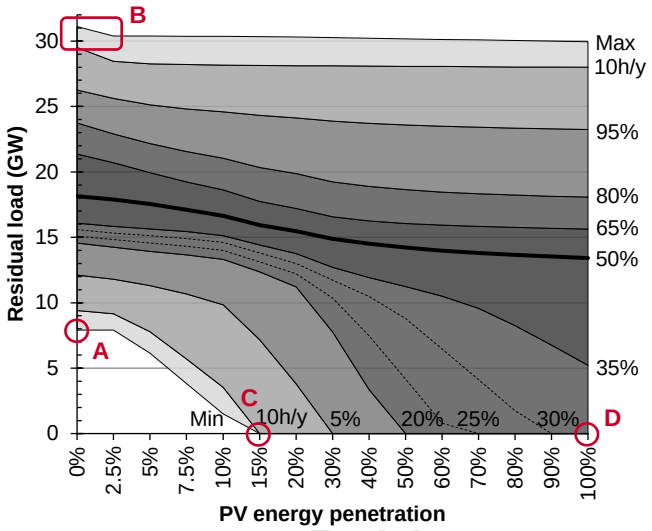

Figure 5: Residual load against PV penetration for different likelihoods of occurrence. Note that the bottom axis is not on scale. Greyscale shading indicates probability distribution of values

decreases with PV penetration at different rates: high values decrease at low penetrations and then tend to asymptotes; low values start steady and then rapidly decrease. The minimum value goes from about 8 GW with no penetration (point A), down to zero with a penetration of 15 % (point C). The maximum value without PV (about 30 GW) decreases about 3.3% with the first step increase of penetration (2.5%, less than the current installed capacity, point B). After this small reduction, the penetration of PV does not significantly affect the capacity adequacy problem. Peak net load decreases at a rate of about 3 MW per GW of installed PV capacity. Even with high penetrations, residual load can be reduced to zero only during a small part of the year. At 100% penetration the residual load is zero for about 32% of time (point D in Figure 5).

Figure 6 considers the effect of PV penetration on residual load from another perspective: the frequency distribution of residual load over different levels of PV penetration. The distribution of load without PV has two peaks: The right

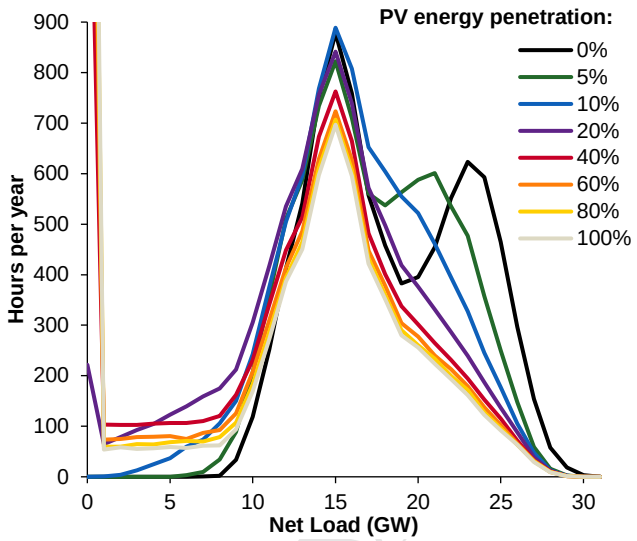

Figure 6: Frequency distribution of the residual load against PV penetration

one corresponds to high load occurring during daytime; the left one to low load occurring at night. The peak related to high daytime load is gradually reduced by the penetration of PV, disappearing for penetrations above 20% (four times the current level). The figure also shows that for high penetrations low values of residual load (0-6 GW) become more common.

Another quantity of interest in simulations with high PV penetration is excess energy or overproduction, i.e. power generated by PV in a given time but would not serve any load of the region Fig.7 shows the annual amount of excess energy for different PV penetrations. In particular, it shows that the absolute values (primary axis) grow faster than linearly with penetrations above 15% (three times the current amount), reaching about 100 TWh per year (more than half of the annual demand) for a 100% penetration. Looking at excess energy as a fraction of the overall PV-generated energy (secondary axis), penetrations

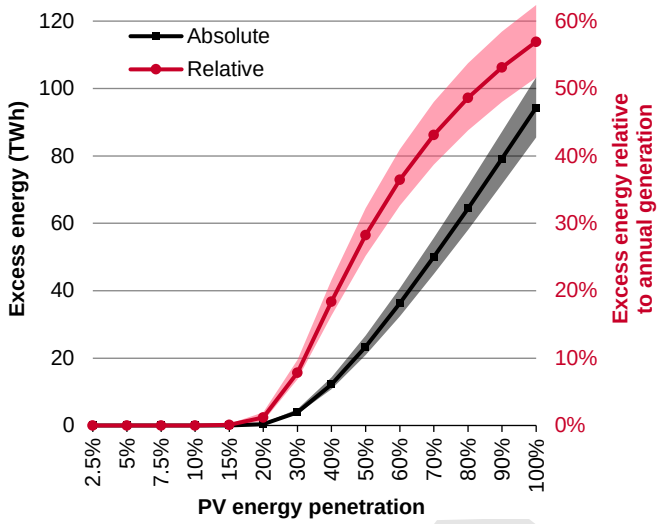

Figure 7: Annual excess generation from PV against PV penetration - minimum, average and maximum. The primary axis (on the left) refers to absolute values [TWh], the secondary axis (on the right) reports the fraction of overall energy generation.

above 15% show an increase, meaning that each additional MW of PV capacity provides less useful energy than the previous MW. Though the marginal increase in relative values is slower than linear for penetrations above 30%, the figure shows that excess energy can reach very high relative and absolute values (about 55% of the generated energy for a PV penetration of 100%). The useful energy produced and thus the value of installed capacity above the 15% penetration limit decreases with penetration unless solutions such as storage, export (if the electricity is needed elsewhere and sufficient inter-regional transmission capacity exists) or demand-side management are employed.

The impact of PV penetration on load faced by non-PV generation can be measured in terms of ramps of the residual load. Fig.8 shows residual load ramps net of excess energy, for different likelihoods of occurrence. There is a degree of symmetry between negative and positive values as ramp-downs and ramp-ups have similar shapes, magnitude and frequencies. Up to a 10% penetration

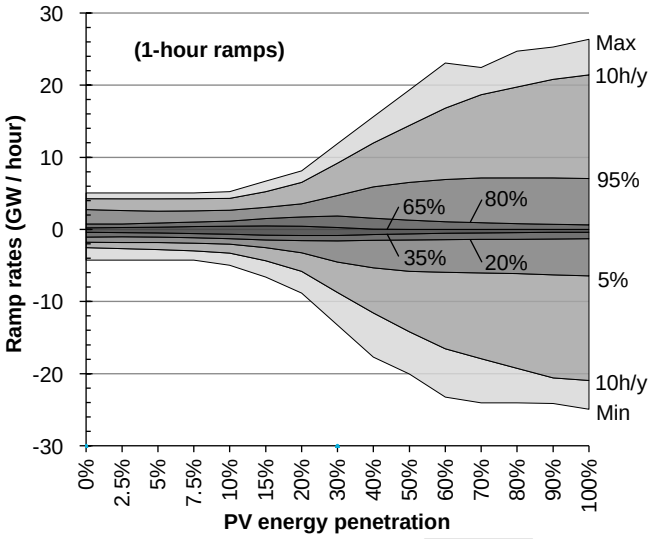

Figure 8: Ramp rates against PV penetration for different likelihood of occurrence.

(twice the current level) the most infrequent ramps are not affected. Their values increase faster than linearly when the penetration is in the range 10-60% and tend to an asymptote starting from a penetration of 60%. At the 100% penetration, absolute values reach about five times the values seen at penetrations below 10% (26 GW/h compared to 5 GW/h). As expected, ramps increase in magnitude but also become more frequent. For example, ramps of about 5 GW/h are seen only infrequently with low penetrations of PV; however, they occur more than 5% of the time for penetrations above 60%.

The reasons behind these results can be better understood with chromatic graphs highlighting the intra-annual variation with different colours. The pattern is similar in each of the ten years, although absolute values differ from year to year. Fig.9 focuses on a single year (2015) to show the residual load net of possible excess energy (RLC) both in case of no PV (above) and in case of 100% penetration (below). The situation of no PV (above) shows clear patterns at different scales: daily (lower values at night), weekly (lower values during weekends) and annual (load is lower during winter holidays and in August; it is

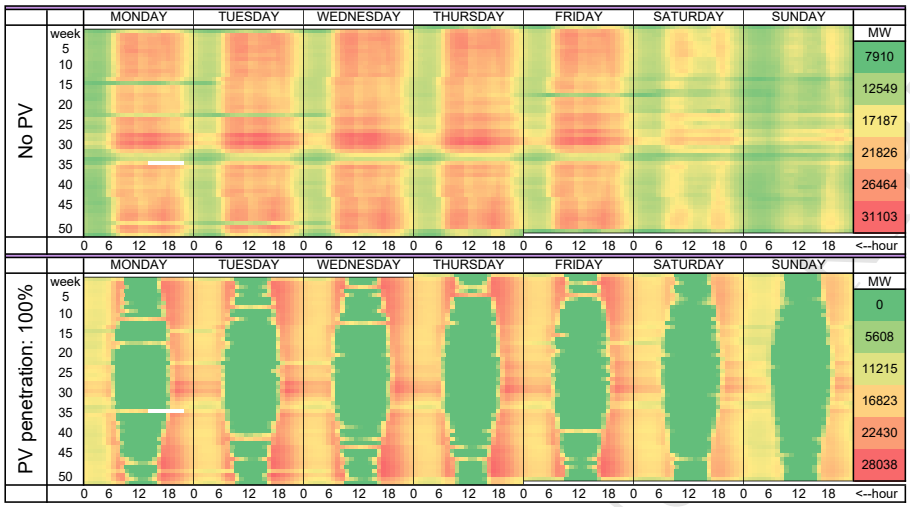

Figure 9: Chromatic graph of the residual load net of the excess energy (RLC) for a selected year (2015) in case of no PV (above) and for a penetration of 100% (below). Red indicates high values while green indicates low values. Note that different color scales have been used for the two charts to highlight dynamics otherwise not visible.

higher in the weeks before August). For a 100% penetration (below), the load is met by the PV generation in the hours around noon, marked in green. No-load situations occur on all days of the week, on almost all days of the year. High values of the residual load are located next to the green areas, mostly in the evening and especially in winter and close to the weeks of the summer peak.

Fig.10 focuses on the hourly ramps (span of 1 hour). Color intensity is proportional to the relative values of each single case (the same color intensity represents the same absolute value within each single case but it does not represent the same absolute value when comparing the two cases). As in the previous chart, several patterns are visible with no PV (above): daily (steep ramp-ups in the morning, gentler ramp-downs in the evening and small valleys around mid-day), weekly (lower values during weekends) and annual. While morning ramp-ups do not change significantly throughout the year, evening ramp-downs are delayed in summer and earlier in winter due to sunset times. The August

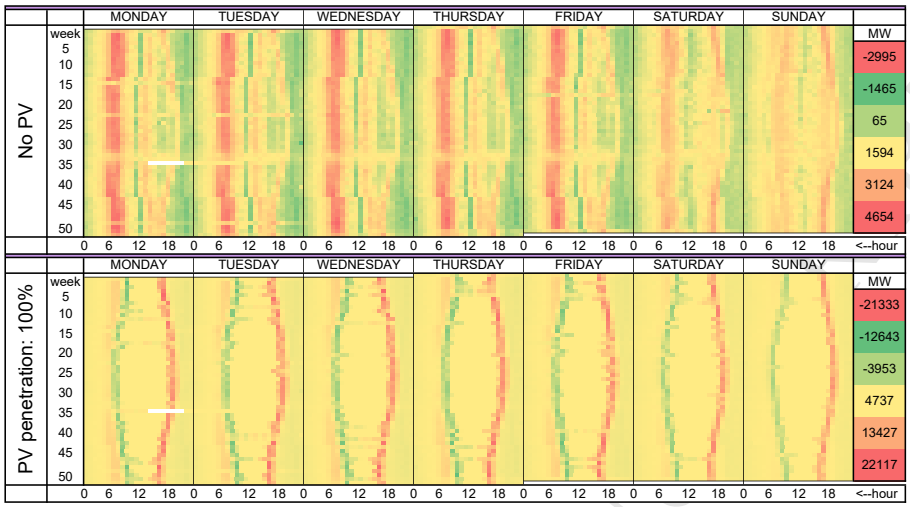

Figure 10: Chromatic graph of the hourly ramp rates of the residual load net of the excess energy (RLC) for a selected year (2015) in case of no PV (above) and for a penetration of 100% (below). Red indicates high values (meaning ramp-ups) while green indicates low values (meaning ramp-downs). Note that different color scales have been used for the two charts to highlight dynamics otherwise not visible.

holidays (which are prominent in Italy) visibly decrease the ramps. With a penetration of 100%, PV generation creates a large valley during the central hours of the day, and ramps are driven primarily by PV. The morning ramp-ups and the evening ramp-downs still exist, but two more important slopes occur between them. The most important ramps in the morning now face downward and the opposite happens for the evening. Since irradiance changes throughout the year, the morning and evening ramps move closer to each other in winter and further apart in summer. Intra-weekly variability is minimal.

Fig.11 shows the evolution of the ramp rates from Fig.8 for different ramp durations, considering different likelihoods of occurrence and different PV penetration levels. For high PV penetrations, the magnitude of infrequent extreme values does not significantly change with the time span covered by the ramp (ramp duration), except when moving from one hour (first graph on the left)

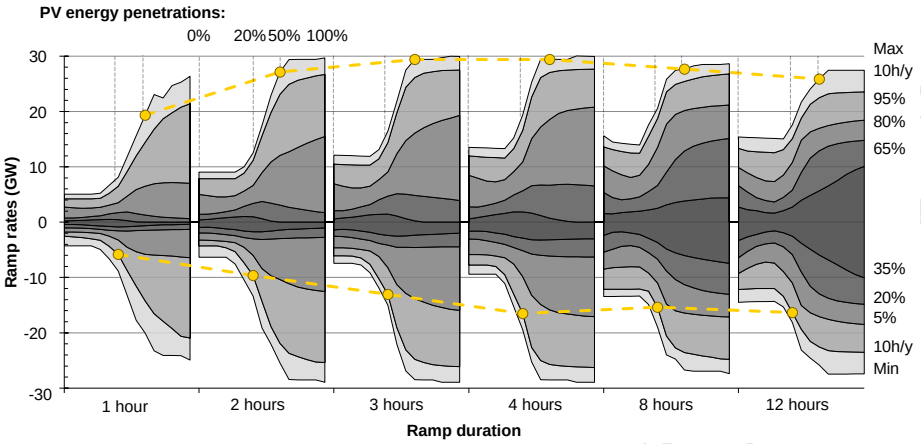

Figure 11: Ramp-ups and ramp-downs, versus PV penetration, for six different ramp durations. The values are reported for different likelihood of occurrence. The two dotted lines link points with the same PV penetration and same likelihood of occurrence across the different durations.

to two hours (second graph). This can be seen by looking at the upper dotted line, which links the maximum values for 50% PV penetration. For low PV penetrations and, in general for low likelihoods of occurrence, ramp values increase consistently with ramp duration. This can be seen by looking at the lower dotted line which links the low values occurring ten times per year with a PV penetration of 20%. The lower the frequency and the penetration, the longer the duration to reach the plateau. The comparison of the six charts shows that extreme ramps do not last more than one hour. In other words, the hours immediately prior to or after the extreme values occurr present ramps with lower magnitude. Ramping rates in the hours adjacent to the most extreme ramps are about one fifth of the extremes in case of very high penetrations; they are about half for lower penetrations.

4.2. Storage requirements

This section analyses the relation between PV penetration and the amount of storage needed to smooth fluctuations in the residual load net of excess energy

(RLC). We analyse eight strategies, averaging RLC over eight different periods: 3, 5, 7, 13, 25, 49, 169 and 721 hours (the last two respectively corresponding to 1 week and 1 month). The effect of the different strategies, resulting in the 8 desired load profiles (DL2) is reported for 100% PV penetration and an example period of two days in Fig.12. Averaging the load over those horizons reduces the

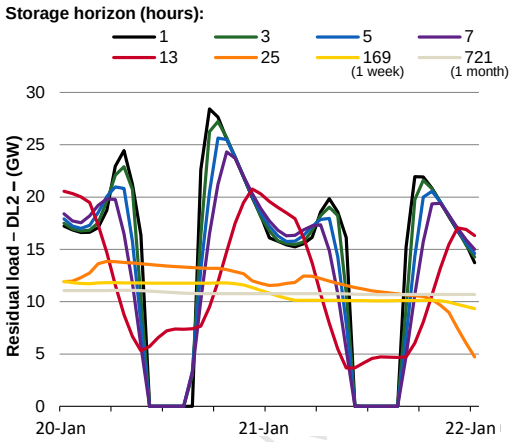

Figure 12: Desired Load (DL2) for the different storage strategies, with a PV penetration of 100%, for an example period of 48 hours.

peaks, the excess energy, and the ramps, as shown in Fig.13, Fig.15 and Fig.14 respectively. From Fig.13, we can see that the maximum residual load decreases with the storage horizon, for any PV penetration. However, the horizon increase barely affects the ability of PV penetration to reduce the peak, except for the one-week and one-month horizons. From the same figure, it is interesting to note also that, while doubling the horizon from 13 hours to 25 hours allows PV penetration to increase of 20% without excess energy curtailment, 721 hours (almost 30 times more) are required for an additional increase of 30%. Storage facilities help to reduce excess energy supply from PV, and their effect varies strongly depending on the storage horizon. From Fig.14, increasing the storage horizon up to 1 day leads to a drastic decrease in excess energy. Increases beyond one day have a limited effect, as this only exploits the difference between

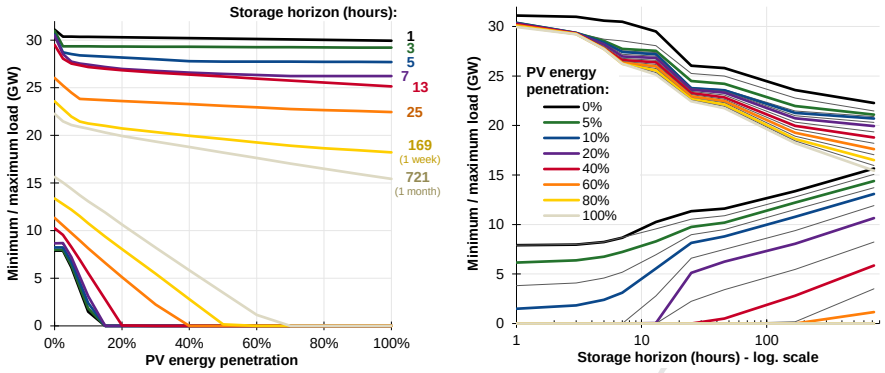

Figure 13: Minimum and maximum residual load for different storage horizons at different PV penetrations.

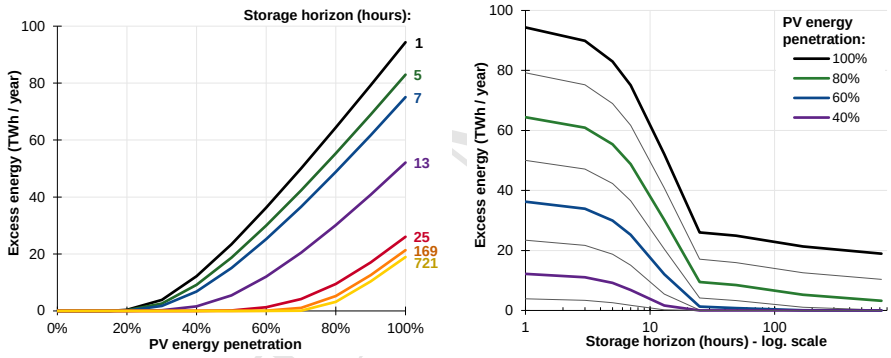

Figure 14: Average annual excess energy for different storage horizons at different PV penetrations.

sunny and cloudy days. The figure also shows that even a storage horizon of 1 month does not avoid an important amount of excess energy with penetrations above 70-80%. Fig. 15 shows the impact of storage on the extreme ramps. Storage reduces the ramps by averaging the load over the different horizons. An important reduction can be seen already with an horizon of three hours. Then, the marginal reduction for every additional hour considered by the storage strategy decreases. Notably, even at 100% penetration, keeping the value of

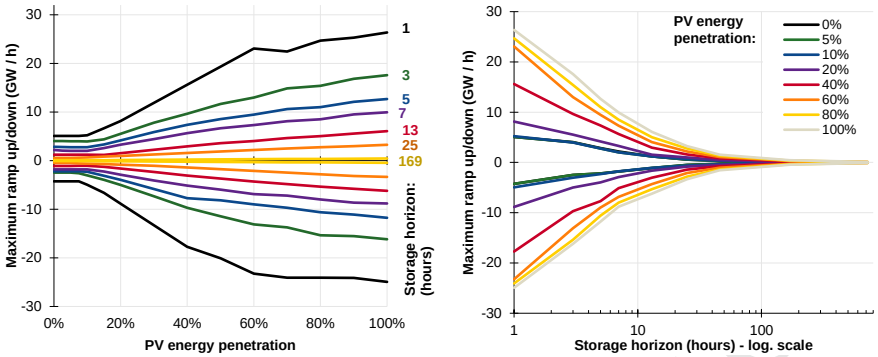

Figure 15: Maximum ramp-up and -down for different storage horizons at different PV penetrations.

extreme ramps as it is in absence of PV requires storage horizons shorter than a day (half a day for penetrations below 80%).

Fig.16 shows the values of three parameters for sizing the storage: (i) the storage capacity (in GWh), (ii) the charging capacity (in GW) and (iii) the discharging capacity (in GW); for different PV penetrations and for different storage horizons. These quantities must be seen as aggregate values referring to the storage facilities possibly deployed in the region. Intuitively, the value of these three parameters generally increases with PV penetration and with the duration of the storage strategy. A noteworthy exception for storage capacity is the assumption of weekly and, in particular, monthly storage horizons: storage capacity decreases until PV reaches a penetration of 15% (see rounded rectangle A), to revert the trend when this latter increases. Overall, the increase of the three parameters is not homogeneous and linear throughout the PV capacity–storage horizon domain.

If we focus on the effect of changing PV penetration (the two charts on the left of Fig.16), for the storage capacity and for the charge and discharge capacities, we can distinguish two different segments of growth, no matter the horizon of the storage strategy. With PV penetration below the range of 10-20% (i.e. when the magnitude of the load and its variations are in the same

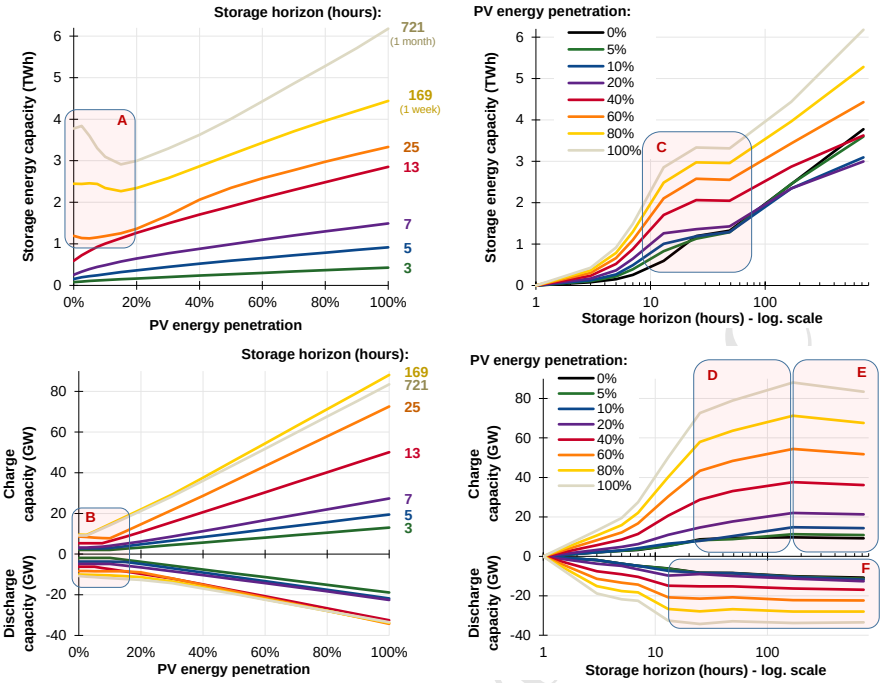

Figure 16: Storage capacity (above), charging and discharging capacity (below) for the storage facilities at different PV penetrations, according to the chosen storage strategies.

order of PV generation and its variations), the 3 parameters show heterogeneous behavior: mostly small increases or even reductions (see rounded rectangle A and B). Greater PV penetrations lead to greater need for storage as the load influence becomes less relevant for the analysis, thus the storage capacity, the charge and the discharge capacity start increasing.

The storage capacity depends on the penetration of PV, and mostly on the storage strategy. Values range from hundreds of GWh (for 3-to-5-hour horizons) to few TWh (from 7-hour horizons on). In the range of 20-100% penetration of PV, the increase is in the order of 2-7 GWh of additional storage per 1 GW_P of PV, for horizons lower than 7 hours, and about 15 GWh of additional storage per 1 GW_P of PV, for horizons greater than 13 hours. An outstanding 26 GWh per GW_P is recorded for the monthly horizon strategy.

With respect to charging and discharging capacities, there is not perfect symmetry in their sizing: for high PV penetration and long horizons, the discharging capacity is less than 40% of the charge capacity; for high PV penetration and short storage horizons, it can be 30% higher than the charge capacity. Depending on the considered horizon, the charging capacity goes from 2 to 10 GW for low PV penetration and from 15 to 90 GW for the highest penetrations. For horizons lower than 7 hours, the charging capacity increases in the range of 0.09-0.17 GW/GW$_P$; for the monthly horizon it increases by around 0.500 GW/GW$_P$. The discharge capacity shows a narrower range of increase compared to the charge capacity: 2-11 GW for penetrations below 10%, 19-23 GW for 100% penetration with short storage horizons, and 33-34 GW for 100% penetration with long storage horizons. For horizons lower than 7 hours, and in the range of 20-100% PV penetration, the discharging capacity increases by 0.13 GW/GW$_P$; for horizons longer than 13 hours it increases by 0.18 GW/GW$_P$.

Focussing on the right side of Fig.16, we again note two different behaviours for the three parameters when the horizon of the storage strategy increases. For storage capacity there is a rapid and approximately linear increase up to the 13-hour horizon; then the growth stops between 13 and 49 hours (see rounded rectangle C) and it increases again with the horizon and the PV penetration. Overall, the marginal increase is higher for short horizons and lower for long ones. This behavior suggests that a large effort (in terms of installing storage capacity) must be made for averaging the residual load within a day. Adding the same amount of capacity increases the horizon over the day, up to a week (on average about 8 GWh of additional storage per each additional hour of the horizon). The need for additional capacity to go over the month is marginally lower, on average about 1-3 GWh of additional storage per each additional hour considered in the horizon.

Similar behavior is seen for charging capacity. Increases up to the 13-25-hour horizon are 0.3-2.6 GW per additional hour, depending on the penetration. Then, the growth consistently slows down for the 49-169 hour horizons (see rounded rectangle D) with an average increase of 0.01-0.1 GW per addi-

tional hour, depending on the penetration. Finally, a decrease is recorded (see rounded rectangle E), when moving from the weekly to the monthly cycles. The discharging capacity depicts a similar trend for short storage horizons, increasing by 0.4 to 2.5 GW per additional hour, depending on the penetration. For horizons greater than 13 hours (see rounded rectangle F), the power does not change significantly with the horizon, due to the fact that the discharge power is mostly driven by the load and does not change with the penetration of PV. This means that a long storage horizon, if considered, might be a limiting factor in terms of storage capacity and charging capacity but would not be so for discharging capacity.

5. Conclusions

The impact of PV penetration on capacity adequacy is highly dependent on the studied region, but some general patterns can be observed. This work contributes to the knowledge of PV penetrations impact on the Italian Nord bidding zone. The findings could help improve design of policies to subsidise and integrate PV in that particular region, and could be relevant when designing the capacity market or other strategies that ensure sufficient reliable capacity is available. Such strategies are likely needed with increasing penetration of variable renewable generation [33]. This is true whether the region is considered as part of the national power system or as part of a future Pan-European electricity market.

Confirming prior work [9], we show that for the analysed region, PV alone cannot significantly contribute the capacity adequacy, even at high levels of penetration. In addition, here we show that storage helps PV to reduce the peak of the residual load. The decrease is nevertheless marginal for storage horizons shorter than a week and limited for longer horizons. Moreover, contribution of PV towards meeting energy demand of the region decreases with penetration due to increasing amounts of excess energy. This potentially leads to losses of 60% of PV production for extremely high penetrations. We find that storage

can help to address this problem, although not eliminate it.

Besides the availability of storage, the actual amount of excess energy would depend on the local demand profile and, according to the degree of interconnection, on the demand outside the region. In our analysis we considered the historical load profile as is, with no flexibility options. Nevertheless, it is likely that, in a hypothetical high PV penetration scenario, the possibility of generating excess energy in some hours at no variable cost would result in low electricity prices on the market in those same hours. This in turn would likely lead to a more flexible demand that could be completely or partially shifted in time, such as space heating (albeit primarily in winter), water heating, refrigeration or charging electric vehicles.

This study reveals new insight beyond the specifics of the case study considered, in particular with respect to long-term ramps in the residual load (demand net of PV output). Like Richardson and Harvey [14] found for Canada, hourly ramps start increasing when penetration rises beyond a certain level. Although their analysis was focused on a lower penetration range, it is interesting to note this finding was replicated despite the different latitude and climatic conditions. The analysis of ramps shows that the steepest ramps do not last for more than a single hour: multi-hour ramps have a lower average rate of change. In particular, the ratio between the slopes of the extreme ramps and the slopes of the preceding or following ones decreases with the penetration of PV. Huber et al. [23] also considered multi-hour ramps, but it is difficult to disentangle the influence of solar PV on their results because of the consideration of wind and solar together. In this work, we find that storage can reduce or eliminate the problem of hourly ramps even with horizons shorter than a day.

In general, our analysis suggests that, although increasing the horizon of the storage strategies over a day leads to marginal benefits, very high PV penetration levels require high charging/discharging and energy capacities of storage. In particular, the charging and discharging capacities needed are one order of magnitude higher than the capacity of pumped hydro storage plants currently installed in the region (about 5 GW of power capacity [34]). Run-of-river or

dam hydro power plants in addition to pumped storage could be one renewable solution in the region (which has low wind power potential) able to help with PV integration, but would not avoid wasting excess energy. Compared to PV, concentrating solar power could avoid excess energy using its built-in storage and could contribute to the reduction of peaks and ramps [35, 36]. However, that requires direct irradiance so would not be suitable for locations with frequent cloud coverage, so concentrating solar power would likely be imported into the Northern Italy region.

The relation between the penetration of variable renewable sources and the implications on capacity adequacy and system security is a primary concern for capacity expansion models. These models cover relatively long time horizons (often, multiple decades) and are therefore not designed to simulate the energy or power system with a fine temporal resolution. In such frameworks, the short-term dynamics due to fluctuations implied by variable sources cannot be detected. Many solutions are adopted to take variable generation into account [37], notably the use of heuristics (e.g. [38]). To use heuristics in a larger model, the modeller needs to analyse variability and its effect a priori [39] (e.g. knowing that installing a certain amount of PV capacity will imply a certain increase of ramp rates). It follows that another important result from this study is that by quantifying the relationship between PV penetration and capacity adequacy - and how this changes with the availability of storage - it enables better modelling of PV for long term planning in the considered region. This approach can easily be replicated for other world regions using the framework presented. In fact, one of the aims of this study is to integrate its results into the linear programming model MELiSsa, a long-term planning tool focused on a particular area within the Nord bidding zone, by constructing piecewise linear relations from the results presented here [40, 41]. Nevertheless, the present study ignores many aspects of power system design, such as the short-term dynamics that characterise the system security problem (i.e. forecast and operating limits implying the need for reserves; lack of rotating inertia implying the need for synthetic inertia or synchronous generation). Building on our analysis, further

work will be able to examine these system constraints in more detail.

In summary, a detailed treatment of solar PV generation, load, and storage is required to properly understand the impacts of PV on capacity adequacy and flexibility requirements. The framework we present can be applied to other world regions to further explore the relationships found here. Notably, we find that even in a Mediterranean climate, solar PV penetration does little to reduce peak capacity requirements and leads to increasing excess energy and increasing ramps in residual load. Storage strategies with horizons longer than a day are important for peak reduction but have a marginal effect on excess energy and are not necessary for ramps. Testing the applicability of these findings in other world regions will be an important next step.

References

[1] REN21, Renewables 2017 global status report, Tech. rep., REN21 - Renewable Energy Policy Network for the 21st Century, Paris: REN21 Secretariat (2017).
URL www.ren21.net/gsr_2017_full_report_en

[2] K. Ogimoto, Power System Operation and Augmentation Planning with PV Integration, Tech. rep., IEA-PVPS (2014).
URL http://www.iea-pvps.org/index.php?id=322%7B&%7Dno%7B_%7Dcache=1%7B&%7Dsword%7B_%7Dlist[]=integration

[3] J. Remund, C. Calhau, L. Perret, D. Marcel, Characterization of the spatio-temporal variations and ramp rates of solar radiation and PV, Tech. rep., IEA-PVPS (2015).
URL http://iea-pvps.org/index.php?id=336&eID=dam_frontend_push&docID=2733

[4] Y.-M. Saint-Drenan, R. Fritz, D. Jost, How an energy supply system with a high PV share handled a solar eclipse, Tech. rep., IEA - PVPS (2016).

URL http://iea-pvps.org/index.php?id=9&eID=dam_frontend_push&docID=3290

[5] ENTSO-E - European Network of Transmission System Operators for Electricity, Scenario outlook & adequacy forecast 2015, Tech. Rep. June, ENTSO-E - European Network of Transmission System Operators for Electricity (2015).
URL https://www.entsoe.eu/Documents/SDC%20documents/SOAF/150630_SOAF_2015_publication_wcover.pdf

[6] R. Green, I. Staffell, Electricity in Europe: exiting fossil fuels?, Oxford Review of Economic Policy 32 (2) (2016) 282–303. doi:10.1093/oxrep/grw003.
URL https://academic.oup.com/oxrep/article-lookup/doi/10.1093/oxrep/grw003

[7] D. Lew, G. Brinkman, E. Ibanez, A. Florita, M. Heaney, B.-M. Hodge, M. Hummon, G. Stark, J. King, S. Lefton, N. Kumar, D. Agan, S. Venkataraman, G. Jordan, The Western Wind and Solar Integration Study Phase 2, Tech. rep. (2013).
URL http://www.nrel.gov/docs/fy13osti/55588.pdf

[8] Atlasole - atlante degli impianti fotovoltaici [cited 2016-12-31].
URL http://atlasole.gse.it/atlasole/

[9] F. Fattori, N. Anglani, J. P. Deane, Implications of the photovoltaic generation on the non-photovoltaic generation in the Lombardy region, in: 2015 IEEE 15th International Conference on Environment and Electrical Engineering (EEEIC), IEEE, 2015, pp. 1391–1396. doi:10.1109/EEEIC.2015.7165373.
URL http://ieeexplore.ieee.org/lpdocs/epic03/wrapper.htm?arnumber=7165373

[10] E. A. Alsema, A. J. M. van Wijk, W. C. Turkenburg, The capacity credit of

grid-connected photovoltaic systems, 5th Photovoltaic Solar Energy Conference -1 (1984) 388–392.
URL http://adsabs.harvard.edu/abs/1984pvse.conf..388A

[11] M. Kaltschmitt, A. Voss, Methodological Approaches for the Estimation of a Capacity Credit of a Grid-connected Photovoltaic Electricity Generation, in: A. Luque, G. Sala, W. Palz, G. Dos Santos, P. Helm (Eds.), Tenth E.C. Photovoltaic Solar Energy Conference, Springer Netherlands, Dordrecht, 1991, pp. pp 486–489. doi:10.1007/978-94-011-3622-8_125.
URL http://link.springer.com/chapter/10.1007%2F978-94-011-3622-8_125

[12] S. Samadi, C. Singh, Capacity credit evaluation of solar power plants, in: 2014 IEEE PES General Meeting — Conference & Exposition, IEEE, 2014, pp. 1–5. doi:10.1109/PESGM.2014.6938831.
URL http://ieeexplore.ieee.org/lpdocs/epic03/wrapper.htm?arnumber=6938831

[13] L. Zhang, Y. Wu, S. Lou, Y. Yang, Y. Wang, Photovoltaic generation capacity credit evaluation method considering its daily output characteristics, in: 2014 International Conference on Power System Technology, IEEE, 2014, pp. 2763–2768. doi:10.1109/POWERCON.2014.6993726.
URL http://ieeexplore.ieee.org/lpdocs/epic03/wrapper.htm?arnumber=6993726

[14] D. B. Richardson, L. Harvey, Strategies for correlating solar PV array production with electricity demand, Renewable Energy 76 (2015) 432–440. doi:10.1016/j.renene.2014.11.053.
URL http://www.sciencedirect.com/science/article/pii/S0960148114007836

[15] F. Groppi, Grid-connected photovoltaic power systems: Power value and capacity value of PV systems, Tech. rep., IEA PVPS (2002).

URL http://hme.ca/gridconnect/IEA_PVPS_Task_5-11_Power_and_Capacity_Value_of_Grid-Connected_PV.pdf

[16] R. Perez, M. Taylor, T. Hoff, J. P. Ross, Reaching Consensus in the Definition of Photovoltaics Capacity Credit in the USA: A Practical Application of Satellite-Derived Solar Resource Data, IEEE Journal of Selected Topics in Applied Earth Observations and Remote Sensing 1 (1) (2008) 28–33. doi:10.1109/JSTARS.2008.2004362.
URL http://ieeexplore.ieee.org/lpdocs/epic03/wrapper.htm?arnumber=4637912

[17] R. Rüther, P. J. Knob, C. da Silva Jardim, S. H. Rebechi, Potential of building integrated photovoltaic solar energy generators in assisting daytime peaking feeders in urban areas in Brazil, Energy Conversion and Management 49 (5) (2008) 1074–1079. doi:10.1016/j.enconman.2007.09.020.
URL http://www.sciencedirect.com/science/article/pii/S0196890407003354

[18] S. Pelland, I. Abboud, Comparing Photovoltaic Capacity Value Metrics: A Case Study for the City of Toronto, Progress in Photovoltaics: Research and Applications 16 (8) (2008) 715–724. doi:10.1002/pip.864.
URL http://doi.wiley.com/10.1002/pip.864

[19] C. Dent, R. Sioshansi, J. Reinhart, A. Wilson, S. Zachary, M. Lynch, C. Bothwell, C. Steele, Capacity Value of Solar Power: Report of the IEEE PES Task Force on Capacity Value of Solar Power, International Conference on Probabilistic Methods Applied to Power Systems (PMAPS), Beijing, China 44 (October 2016).

[20] S. Pfenninger, I. Staffell, Long-term patterns of European PV output using 30 years of validated hourly reanalysis and satellite data, Energy 114 (2016) 1251–1265. doi:10.1016/j.energy.2016.08.060.

[21] P. Denholm, R. Margolis, Energy Storage Requirements for Achieving 50 % Solar Photovoltaic Energy Penetration in California, Tech. Rep. August,

NREL National Renewable Energy Laboratory (2016).
URL www.nrel.gov/docs/fy16osti/66595.pdf

[22] ENTSO-E - European Network of Transmission System Operators for Electricity, Mid-term Adequacy Forecast 2016 edition, Tech. rep. (2016).
URL https://www.entsoe.eu/outlooks/maf/Pages/default.aspx

[23] M. Huber, D. Dimkova, T. Hamacher, Integration of wind and solar power in Europe: Assessment of flexibility requirements, Energy 69 (2014) 236–246. doi:10.1016/j.energy.2014.02.109.

[24] P. Denholm, R. M. Margolis, Evaluating the limits of solar photovoltaics (PV) in electric power systems utilizing energy storage and other enabling technologies, Energy Policy 35 (9) (2007) 4424–4433. doi:10.1016/j.enpol.2007.03.004.
URL http://www.sciencedirect.com/science/article/pii/S030142150700095X

[25] L. Koh, G. Z. Yong, W. Peng, K. Tseng, Impact of Energy Storage and Variability of PV on Power System Reliability, Energy Procedia 33 (2013) 302–310. doi:10.1016/j.egypro.2013.05.071.
URL http://www.sciencedirect.com/science/article/pii/S1876610213000817

[26] T. Weiss, A. Lucken, D. Schulz, An empirical approach to calculate short and long term energy storage needs of an electricity system, in: 2013 48th International Universities' Power Engineering Conference (UPEC), IEEE, 2013, pp. 1–6. doi:10.1109/UPEC.2013.6714953.
URL http://ieeexplore.ieee.org/lpdocs/epic03/wrapper.htm?arnumber=6714953

[27] M. G. Prina, G. Garegnani, D. Kleinhans, G. Manzolini, R. Vaccaro, S. Weitemeyer, D. Moser, Large-Scale Integration of Renewable Energy Sources : Technical and Economical Analysis for the Italian Case, in: 32nd

European Photovoltaic Solar Energy Conference and Exhibition, no. June, 2016, pp. 2670 – 2674.
URL http://www.eupvsec-proceedings.com/proceedings?paper=37326

[28] R. Müller, U. Pfeifroth, C. Träger-Chatterjee, R. Cremer, J. Trentmann, R. Hollmann, Surface solar radiation data set - heliosat (SARAH) - edition 1 (2015).
URL http://dx.doi.org/10.5676/EUM_SAF_CM/SARAH/V001

[29] R. Müller, U. Pfeifroth, C. Träger-Chatterjee, J. Trentmann, R. Cremer, Digging the METEOSAT treasure—3 decades of solar surface radiation, Remote Sensing 7 (6) (2015) 8067–8101. doi:10.3390/rs70608067.
URL http://www.mdpi.com/2072-4292/7/6/8067

[30] Regione Lombardia - Ente Regionale per i Servizi all'Agricoltura e alle Foreste, Uso del suolo in Regione Lombardia - Atlante Descrittivo, Tech. rep. (2010).
URL http://www.ersaf.lombardia.it/upload/ersaf/pubblicazioni/AtlanteUsoDelSuolo2010_13383_391.pdf

[31] Terna S.p.A., Transparency report - Actual load data [cited 2016-12-31].
URL http://www.terna.it/en-gb/sistemaelettrico/transparencyreport/load/actualload.aspx

[32] ENTSO-E - European Network of Transmission System Operators for Electricity, Production, Consumption, Exchange Package [cited 2016-12-21].
URL https://www.entsoe.eu/db-query/country-packages/production-consumption-exchange-package

[33] A. Botterud, G. Doorman, Generation investment and capacity adequacy in electricity markets, International Association for Energy Economics. ... (2008) 877–884doi:10.1145/1982185.1982376.

URL http://doi.acm.org/10.1145/1982185.1982376%5Cnhttp://www.iaee.org/documents/newsletterarticles/208Botterud.pdf

[34] A. Frigerio, M. Meghella, G. Bruno, Valutazione del potenziale dei sistemi di accumulo di energia mediante centrali di pompaggio idroelettrico per il sistema idroelettrico italiano Analisi di fattibilità preliminari, Tech. rep., RSE Ricerca Sistema Energetico (2012).
URL https://abalderi.files.wordpress.com/2015/06/studioaccumuloidraulico-rse2012.pdf

[35] S. H. Madaeni, R. Sioshansi, P. Denholm, Estimating the Capacity Value of Concentrating Solar Power Plants With Thermal Energy Storage: A Case Study of the Southwestern United States, IEEE Transactions on Power Systems 28 (2) (2013) 1205–1215. doi:10.1109/TPWRS.2012.2207410.
URL http://ieeexplore.ieee.org/document/6266722/

[36] S. Pfenninger, P. Gauch, J. Lilliestam, K. Damerau, F. Wagner, A. Patt, Potential for concentrating solar power to provide baseload and dispatchable power, Nature Climate Change 4 (8) (2014) 689–692. doi:10.1038/nclimate2276.
URL http://www.nature.com/doifinder/10.1038/nclimate2276

[37] S. Collins, J. P. Deane, K. Poncelet, E. Panos, R. C. Pietzcker, E. Delarue, B. P. Ó Gallachóir, Integrating short term variations of the power system into integrated energy system models: A methodological review, Renewable and Sustainable Energy Reviews 76 (2017) 839–856. doi:10.1016/j.rser.2017.03.090.
URL http://www.sciencedirect.com/science/article/pii/S1364032117304264

[38] M. Welsch, M. Howells, M. R. Hesamzadeh, B. Ó Gallachóir, P. Deane, N. Strachan, M. Bazilian, D. M. Kammen, L. Jones, G. Strbac, H. Rogner, Supporting security and adequacy in future energy systems: The need to enhance long-term energy system models to better treat issues related to

variability, International Journal of Energy Research 39 (3) (2015) 377–396. doi:10.1002/er.3250.
URL http://doi.wiley.com/10.1002/er.3250

[39] S. Pfenninger, A. Hawkes, J. Keirstead, Energy systems modeling for twenty-first century energy challenges, Renewable and Sustainable Energy Reviews 33 (2014) 74–86. doi:10.1016/j.rser.2014.02.003.
URL http://www.sciencedirect.com/science/article/pii/S1364032114000872

[40] F. Fattori, D. Albini, N. Anglani, Proposing an open-source model for unconventional participation to energy planning, Energy Research & Social Science 15 (2016) 12–33. doi:10.1016/j.erss.2016.02.005.
URL http://linkinghub.elsevier.com/retrieve/pii/S2214629616300160

[41] F. Fattori, N. Anglani, An Instrumental Contribution to Include the Impact of PV on Capacity Adequacy in Long-Term Energy Models, in: 17th International Conference on Environment and Electrical Engineering (EEEIC), IEEE, 2017.

A. Appendix A

Appendix A describes how we built the final load time series used in the analysis. Four operations were needed: (i) removing erroneous values from the two sources of data (ENTSO-E and Terna), (ii) synchronising the series, (iii) filling the gaps within the ENTSO-E series, and (iv) building the missing data from Terna. These four points are respectively described in detail in the following sections.

A.1. Removing erroneous data

Three different types of erroneous values were found (see Fig.A.1): (i) outliers located at the point of switching from standard time (UTC+1) to Daylight

Saving Time (DST, UTC+2); (ii) outliers that had no systematic distribution; (iii) strings of few hours inconsistent with the mean behavior of the profile in same conditions or inconsistent with the other series. The erroneous values

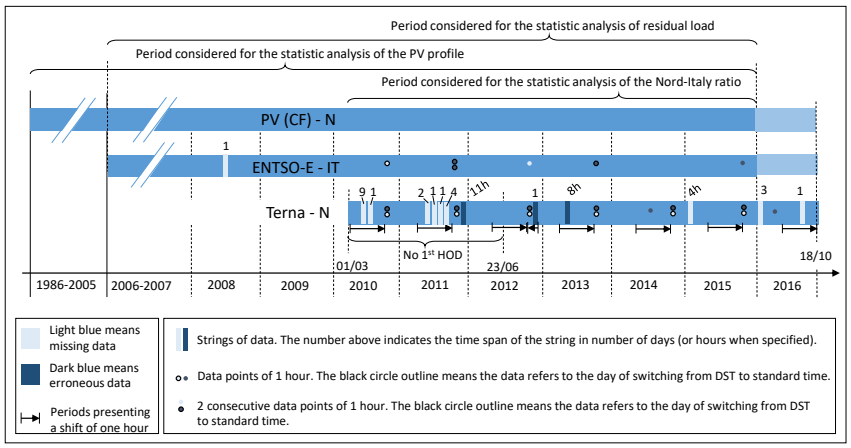

Figure A.1: Qualitative representation of the availability of the data-series which the work is based on: (i) PV capacity factor of the Nord bidding zone; (ii) Italian aggregate of load from ENTSO-E; (iii) load of the Nord bidding zone from Terna. Missing and erroneous data are highlighted in the representation.

of the first two types were detected by filtering high values of the differences from hour to hour whereas in the third case the erroneous values were detected through the difference between the national profile of Terna and ENTSO-E. In all the three cases the detected erroneous values went through visual inspection before being removed.

A.2. Synchronising time series

The load series of Terna had systematically to be time-shifted for the periods of Daylight Saving Time to be synchronous with the ENTSO-E series. The opposite situation was found in a single case right after switching from the DST to the standard time, for a limited period of few days. (see Fig.A.1)

A.3. Filling gaps

Gaps, namely periods of missing data or period of removed erroneous values, were found in the load series of both sources. ENTSO-E's national load series presented few negligible gaps: (i) five single data points of one hour (in one case two consecutive hours) and (ii) a string of 24 hours. In the first case a linear interpolation was used between the previous and the following hours. We can assume this does not affect the analysis since resulting profiles are consistent with the mean behavior and moreover they occur in hours of no PV generation. In the second case, each hour of the string is the average between the same hour of the day before and the same hour of the day after. Again, we can assume this does not affect the analysis because the resulting profile considering the previous and the following days (d-1:d+1) is consistent with the mean behavior of the same portion of week of the same year and with the mean behavior of the same portion of week in the same week of other years. Terna's load series for the Nord bidding zone is characterised by more missing data compared to ENTSO-E. In particular: (i) 12 strings of data ranging from few consecutive hours up to 9 consecutive days; (ii) single data points of one hour referring to the first hour of each day for more than two years; (iii) 6 single data points of two hours located at the point of shifting from standard time to DST; (iv) 2 single data points of one hour with no systematic time distribution. As with ENTSO-E's series, missing data points of one or two consecutive hours were replaced by linear interpolation between the previous hour and the following one; strings of 4 hours up to 1 day were replaced by the average value of the same hour between the previous day and the following one. Longer gaps were modelled using a regression from the ENTSO-E national series, as described in the following section.

A.4. Building synthetic Nord time series

The missing years of the Nord load profile (January 2005 to March 2010) and the four periods of missing data spanning more than a day were modelled based on ENTSO-E series. We started by analysing the ratio between the Nord load

profile provided by Terna and the national load profile provided by ENTSO-E. The ratio was calculated for each t-th hour for which both values were available (and not erroneous) to create a series as in:

$$R_t = LNord_t / LIta_t \tag{A.1}$$

where $LNord_t$ is the load series of the Nord bidding zone, by Terna, and $LIta_t$ is the national load series, by ENTSO-E.

On average, load in Nord is 51.17% of the Italian total, however this ratio varies systematically with time: as depicted in Fig.A.2, load in Nord is relatively lower than the national average on weekends, overnight and during national holidays.

The simplest method of estimating Nord demand from the Italian total is to assume that Nord always consumes 51.17% of the national total. We improve the estimation by using coefficients that account for the temporal variations depicted in Fig.A.2. Knowing the date and hour each j-th value refers to (UCT+1 reference), we define three different coefficients based on the day of week (RDOW), hour of day (RHOD), and day of year (RDOY), respectively:

$$RDOW_i = \overline{R}_t \forall t \in A_i, \forall i \in [1:7] \tag{A.2}$$

$$RDOY_j = \overline{R}_t \forall t \in B_j, \forall j \in [1:365] \tag{A.3}$$

$$RHOD_k = \overline{R}_t \forall t \in C_k, \forall k \in [1:24] \tag{A.4}$$

where A_i, B_j and C_k are the sets of hours of the considered time-period (2010-2015) that can be respectively assigned to the *i-th* day of the week, the *j-th* day of the year[4], and the *k-th* hour of the day[5]. To produce the improved

[4]For leap years, the calculation considers both the 28th and the 29th of February as the 59th day of the year

[5]Since the mean daily profile of the ratio was slightly different during standard time and

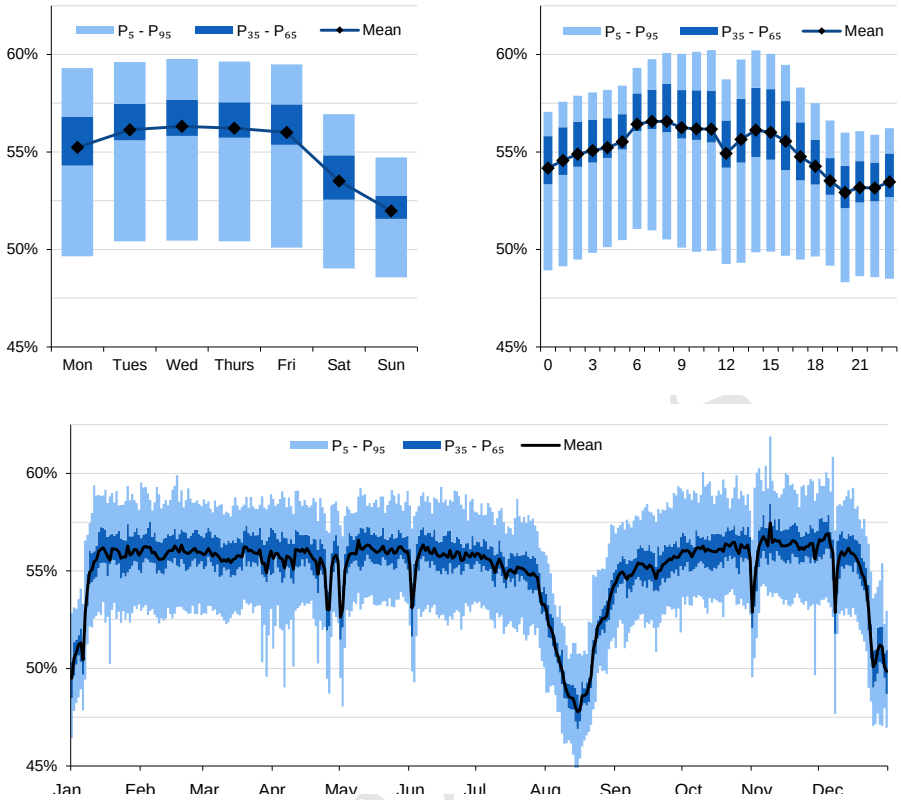

Figure A.2: Ratio between the Nord load and the national load for the year 2015, with respect to day of week, hour of day, and day of year.

estimation of the Nord load profile for 2006-2010, these three coefficients were normalised for each single hour, multiplied together and then multiplied by the overall average ratio (51.17%) and by the national value of that same hour:

$$ELNord_t = \frac{RDOW_i}{\overline{RDOW}_i} \cdot \frac{RHOD_j}{\overline{RHOD}_j} \cdot \frac{RDOY_k}{\overline{RDOY}_k} \cdot \overline{R}_t \cdot LIta_t \qquad \text{(A.5)}$$

where $ELNord_t$ is the estimated load for the Nord zone in the t-th hour.

L_t, the series used in eq.1 for calculating residual load, is finally obtained by putting in sequence the $ELNord_t$ and $LNord_t$ series (the latter cleaned and

DST, we actually considered two different subsets of C_k, one for days of Standard Time and one for days of DST

fixed as explained in the previous sections).

Highlights

- We analyse combinations of PV penetration and storage capacity in Northern Italy
- High penetrations of PV do not reduce peak demand and strongly increase ramp rates
- A large amount of PV generation is potentially wasted at high PV penetrations
- Storage helps to reduce the peak, limits ramps and excess energy generation
- An infeasibly large storage capacity is needed to accommodate high penetrations